Frequency Resolved Angle and Time Difference of Arrival Estimation With Spatial Spectral Holography

R. Krishna Mohan, Z. W. Barber, C. Harrington and W. R. Babbitt
Spectrum Lab, Montana State University, Bozeman, MT 59717, USA
krishna@spectrum.montana.edu

Abstract: Correlative power spectrum and spectral phase mapping via readout of a fiber interferometer with spatial-spectral materials is analyzed and demonstrated to enable precise frequency resolved time delay and angle of arrival estimation with microwave signals.

OCIS codes: (070.1170) Fourier optics and signal processing : Analog optical signal processing; (090.2900) Holography: Optical storage materials

1. Introduction

Rapid determination of a signal's location is used by modern electronic warfare systems and applications to either queue other sensors or employ countermeasure responses. One important parameter needed to identify and locate the sources of hostile electronic signals is the angle of arrival (AOA), or equivalently the time difference of arrival (TDOA) information. Modern military applications require high accuracy AOA measurement systems and signal intercept methods that can capture and process multiple signals with complex modulation formats, ultrawide bandwidth, and fast response, and simultaneously perform precise phase mapping over a wide frequency band.[1]

Here we develop the concept of AOA measurement based on correlative wideband spectrum analysis and processing utilizing a photonic processing device where the RF/microwave signals from the antenna are up-converted onto an optical carrier and monitored, captured, and read out with spatial-spectral (S2) optical materials. The recording of the power spectrum as well as the relative phase of the incoming RF signals is made possible by use of a fiber Mach-Zehnder (MZ) geometry with electro-optic modulators (EOM) that enables spectral identification and direction finding of signal sources. Since this interferometric technique utilizes the phase of the spectral interference, it works on signals with broadband spectra or sparse spectra or even single RF tones. In addition, it works for transient non-repetitive signals, for which there are no spectrum analysis methods with as much resolving power (i.e. number of spectral bins) or resolution (e.g. < 1 MHz) as S2 material based spectral analyzers.

A Rare-earth-ion-doped crystal that is capable of recording broadband optical power spectra with fine resolution is at the core of a S2 based optical signal processor. The individual dopant ions in the crystal have optical resonances with exceptionally narrow linewidths (~kHz) at cryogenic temperatures (4 to 6 K). Inhomogenoeus broadening of the overall absorption profile to several tens of GHz is caused by microscopic inhomogeneities in the crystal that shift and randomly distribute the resonant frequencies. Inhomogeneous to homogeneous bandwidth ratios as large as 10^8 have been reported [2], which provide the large time-bandwidth product essential for several signal processing applications. Thulium and Erbium doped hosts (~10^{18} ions per cm^3) such as YAG and $LiNbO_3$ have been used to demonstrate several analog signal processing capabilities such as spectrum analysis [3], range Doppler processing [4,5], analog to digital conversion [6], and true time delay generation [7].

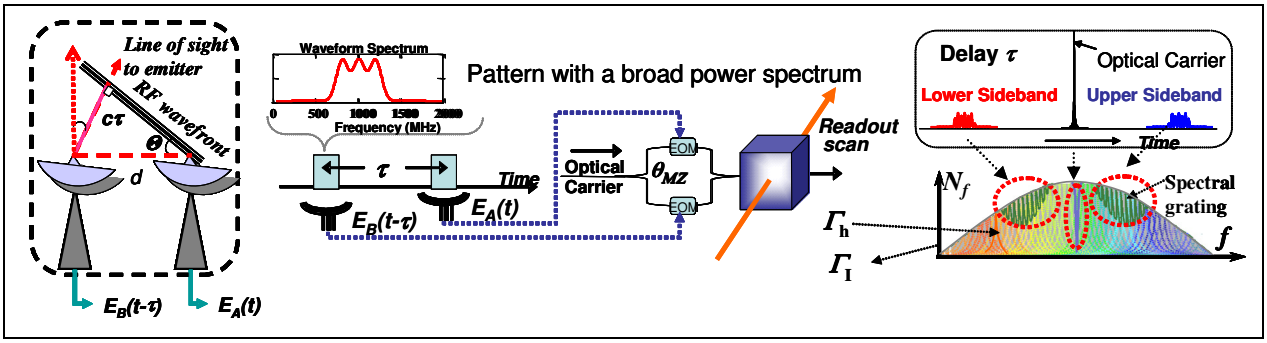

Fig. 1 Schematic of the Angle of Arrival estimation with S2 materials and MZ Inteferometer Demonstration of the spectral grating concept using broadband RF waveforms.

2. Concept and theory

In this section the concept of correlative spectral processing and the principle of TDOA estimation are presented. The schematic for the demonstration is shown in Fig. 1. The demonstration of the ability to estimate time difference of arrival of microwave signals received by a phased array antenna is carried out with a correlative spectral receiver based on a cryogenic Tm:YAG crystal that operates on ultrawide bandwidth microwave signals modulated onto a stabilized optical carrier at 793 nm (frequency doubled Koheras). A MZ fiber interferometer is configured with a 20 GHz electro-optic phase modulator (EOSpace) in each arm, which are utilized to modulate the optical carrier. The optical output of the MZ EOM interferometer is amplified with a semiconductor optical amplifier (500 mW, BoosTA). The interferometric setup is configured to operate at quadrature ($\theta_{MZ}= \pm\pi/2$). The fiber path lengths are actively stabilized with an in-line fiber stretcher using servo feedback. The RF patterns drive the two EOMs in the MZ interferometer and are modulated onto the optical carrier. The S2 material can be programmed with both outputs of the MZ spectral interferometer, which is advantageous when the contrast and the bias of the interferometer is non-ideal. In the current demonstrations a single port output of the MZ interferometer is used to program the S2 crystal. The programmed spectral gratings are read out for each time delay with a wideband optical chirp in a non-collinear geometry. A fraction of the optical chirp is transmitted through the S2 crystal to be used as a reference beam for balanced detection. The resultant balanced output of the detector is digitized and post-processed to yield sinusoidal signals that can be used to estimate the time delay.

Here we present the theory of a spectral interferometer that is assumed to operate at quadrature ($\theta_{MZ} = \pm\pi/2$) with ideal contrast (η=1). Using the theory of MZ interferometry the powers at the upper and lower sideband optical components of interest at any frequency ω_R can be evaluated as

$$P_{1+} = |\beta(\omega_R)|^2 E_0^2 \left(1 + \sin\left(\omega_R \tau\right)\right)/2$$
$$P_{1-} = |\beta(\omega_R)|^2 E_0^2 \left(1 - \sin\left(\omega_R \tau\right)\right)/2 \qquad (1)$$

The difference of the sideband powers yields the phase spectrum of the RF signals while the sum provides the power spectrum. Thus the ratio of the difference to the sum of the sideband powers normalizes the phase spectrum and enables the extraction of the desired time delay independent of the RF power at ω_R. From Eq. (1) we get

$$S_1 = \frac{P_{1+} - P_{1-}}{P_{1+} + P_{1-}} = \sin(\omega_R \tau) \qquad (2)$$

Note that this technique allows the time delay to be estimated using only one spectral component of the input rf signal. In general, the ratio of the difference to the sum (cf. Eq (2)) of sidebands can be written as $S_1(\omega) = \sin(\omega\tau(\omega))$, which indicates that the estimation of the time delay $\tau(\omega) = \sin^{-1}(S_1(\omega))/\omega$ between the two antenna outputs can be carried out for each RF frequency component independently. Thus, multiple temporally simultaneous and spectrally non-overlapping RF signals from different directions can be spectrally distinguished and located. A general theory for time delay estimation when the interferometer has non-ideal contrast and operates away from quadrature and a technique for using the light and dark ports to improve performance have been developed.

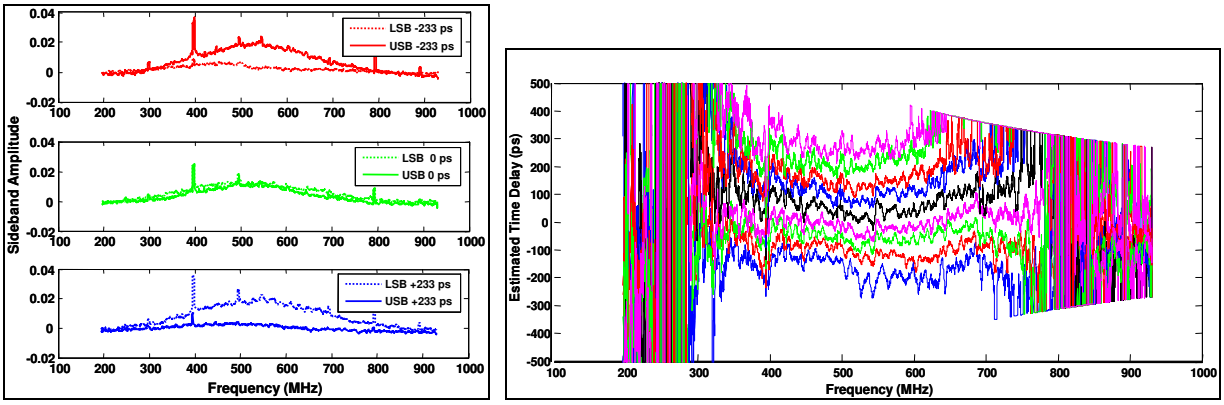

Fig. 2 (Left) Upper and lower sideband spectra at zero time delay and symmetric finite time delays. The change in the sideband amplitude with time delay can be seen. (Right) Time delay estimation using $\arcsin(S(\omega))/\omega$ function over the entire RF waveform bandwidth. The time-delays extracted with 50 ps delay resolution are shown. For ideal operation (($\theta_{MZ} = \pi/2$, $\eta = 1$) extracted delay should be a straight line. The deviations from ideality could be accounted for with non-unity contrast.

3. Demonstrations and analysis

For the demonstrations presented here, the RF waveforms, spanning 400 – 800 MHz, used to drive the EOMs were generated with an arbitrary waveform generator (Tektronix AWG 7102) and the time delays were generated with a mechanical phase shifter (Aeroflex/Weinschel in-line trombone). For every programmed time delay the output of the optical chirp was detected and digitized. The extracted lower and upper sidebands for different time delays are shown in Fig. 2. It can be seen that the sideband amplitudes vary with the time delay as expected. For example, at zero time delay the argument of the arcsin function has to be zero implying that the phase spectrum is zero or equivalently the sideband powers should be equal as seen in the figure. The ratio of the difference to the sum of the sidebands is utilized to extract the time delay of interest.

To estimate the performance of the TDOA system, a comparison between the time delays obtained using the approach described above and the programmed time delays was made. Significantly, it should be noted that the time delays were extracted over the entire bandwidth in a single capture. Fig. 3 shows the average of estimated time-delays over the 450-600 MHz spectral region for every programmed time-delay. The rms error of the delay estimation was measured to be ~ 16 ps. This corresponds to a phase resolution of about 1.8^{o} for an RF frequency component at 500 MHz, over a total demonstrated unambiguous field of view of $\lambda/4$. (±250 ns).

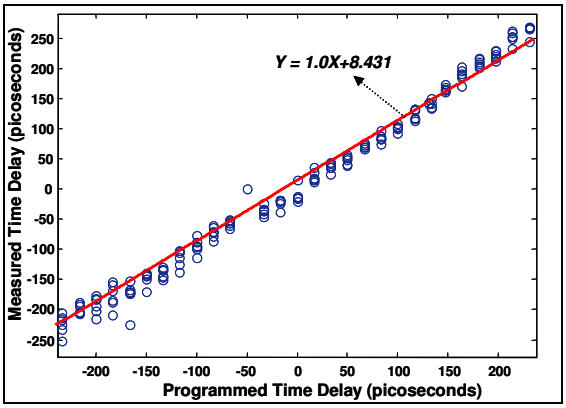

Fig. 3 Time delay estimation using the arcsin(S(ω))/ω function.. Data collected over several independent captures is shown. The RMS error in the delay estimation is about 16 ps for data between 450-600 MHz captured with 100 kHz resolution.

4. Summary and Acknowledgements

We have presented a novel technique based on phase sensitive spectral correlation in a fiber MZ interferometric configuration that enables spectrally resolved estimation of time differences of arrival. The S2 material based spectral correlator measures the spectral power and differential phase of microwave signals, regardless of modulation format. An analytical theoretical model has been presented for the processing of the upper and lower sideband spectra that are recorded for in the S2 material and readout with a chirped optical beam. A proof of concept demonstration has been carried out with RF waveforms modulated onto optical carriers at 793 nm and a Tm:YAG crystal. This work has supported by the Office of Naval Research (contract No. N66001-09-C-2002).

5 References

[1] Electronic Warfare and radar engineering systems handbook, Naval Air Systems Command (1999); Introduction to electronic warfare modeling and simulation, David L. Adamy, SciTech Publishing, (2006)

[2] G.M. Wang, R.W. Equall, R.L. Cone, M.J.M. Leask, K.W. Godfrey, and F.R. Wondre, Opt. Lett. 21, (1996) 818

[3] R. K. Mohan, T. Chang, M. Tian, S. Bekker, A. Olson, C. Ostrander, A. Khallaayoun, C. Dollinger, W. R. Babbitt, Z. Cole, R.R. Reibel, K. D. Merkel, Y. Sun, R. Cone, F. Schlottau, K. H. Wagner, "Ultra-wideband spectral analysis using S2 technology, Jl. of Lumin., 127, 116 (2007)

[4] K.D. Merkel, R. Krishna Mohan, Z. Cole, T. Chang, A. Olson, and W. R. Babbitt, "Multi-Gigahertz radar range processing of baseband and RF carrier modulated signals in Tm:YAG," J. Lum. 107, 62-74, 2004;

[5] T. L. Harris, K. D. Merkel, R. K. Mohan, T. Chang, Z. Cole, A. Olson, and W. R. Babbitt, "Multigigahertz range-Doppler correlative signal processing in optical memory crystals," Applied Optics, 45(2), 343-352, 2006

[6] R. R Reibel, C. Harrington, J. Dahl, C. Ostrander P. Roos, T. Berg, R. Krishna Mohan, M. Neifeld, W.R. Babbitt, "Demonstrations of analog-to-digital conversion using a frequency domain stretched processor", Optics Express, Vol. 17 Issue 14, pp.11281-11286 (2009)

[7] R. Reibel, Z.W. Barber, J. Fischer, M. Tian, W.R. Babbitt, "Broadband Demonstrations of True-Time Delay Using Linear Sideband Chirped Programming of Optical Coherent Transients", J. of Lumin. 107, 103-113 (2004)